.....

Galactic Molecular Clouds and Their Place in the Galaxy
A PhD Literature Review

.....

Lee James Summers

January 2009

Contents

Introduction

Any study of star formation must include an understanding of Molecular Clouds (MCs). MCs are the sites where all known star formation is thought to occur, hence whenever an area containing young stars reside, it is assumed that one will also find a MC, Blitz & Williams (1999). Knowledge of these stellar birthplaces assist in not only in models of stellar but also Galactic evolution, Larson (1981); Glover & Mac Low (2007). This report details the main and current understanding of various forms of MC, what observations and detections are carried out and obtained and how these data can be used to determine the physics of clouds.

Chapter 1 of the review begins by detailing a regime by which the different types of clouds may be classified and the main characteristics of each. We then move on in chapter 2 to the physical and chemical processes within the clouds themselves; which elements are formed, how they are formed and the reactions through which they decay. The main constituents of the clouds are then defined and how these molecules are detected. Finally the chapter 3 details how and which molecular transitions are used to determine the physical attributes of a cloud; including Mass, Kinetic Temperature and the Magnetic Field. Chapter 4 concludes with a statement of initial intent with regards to the direction of the current research .

Chapter 1

Galactic Molecular Clouds

Galactic molecular clouds may be split into four different classes; *Diffuse, Giant Molecular, Dark* and *Dense Clouds* (*Bok Globules* being a sub-class of this catagory), with decreasing levels of internal motion. Within the Dark cloud category, there also exists two further sub-classes of denoting their general environment, that being *Individual* or *Complex*. The general physical properties of these (sub-)classes of cloud are presented in Table 1.1 below;

Cloud Type	A_v (mag)	n_{tot} (cm^{-3})	L (pc)	T (K)	M ($M_\odot$)	Example
Diffuse	1	500	3	50	50	ζ Ophiuchi
Giant Molecular	2	100	50	15	10^5	Orion
Dark						
Complex	5	500	10	10-25	10^4	Taurus-Auriga
Individual	10	10^3	2	10	30	B1
Dense	10	10^4	10^{-1}	10	10	TMC-1/B335

Table 1.1: Physical Attributes of Galactic Molecular Clouds

Table data courtesy of Stahler & Palla (2004)

Where A_v is the average visual extinction along the line of sight the through the cloud interior, L is the cloud's diameter, n_{tot} being the space averaged number density of the cloud, T is the cloud's temperature in Kelvin and M being the characteristic mass of the cloud in units of solar mass. It is important to note that with any classification system

similar to that detailed in table 1.1, there must be a degree of arbitrariness. The best example of this being the quantity labeled L, it is often the case that the parameter is just a representation of an averaged discrete value within a range which often overlaps with its neighbouring classification types. So it is better to think of these parameters as typical guidelines for the clouds rather than absolute rules that govern them.

1.1 Diffuse Clouds

The first classification we shall consider are the *Diffuse Molecular Clouds* (DMCs). The DMCs contain comparable, by number density, amounts of both atomic and molecular Hydrogen, though *Table 1.2* further defines these charateristics. Its close to unity extinction means that background radiation can easily traverse the areas which these clouds occupy, allowing us to detect the absorption lines within the radiation giving rise to information not only with regard to the molecular compositions of the clouds but also the chemical reactions within.

Given the mean density of the Interstellar Medium (ISM) was significantly lower than any laboratory vacuum, early astronomers were surprised to find that the ISM in fact harboured molecules (Snow & McCall (2006)). Early High-Resolution spectroscopic imaging, conducted by the Mount Wilson and Dominion observatory in the 1930s, found that the ISM contained, not just traces, but abundances of molecular gas. These were found by analysing the optical absorption lines from several background stars. The molecules found were CH, CN and CH^+(Snow & McCall (2006)). Snow & McCall (2006) devised a sub-classification system for the DMCs which will be employed here as a framework for discussion; The very nature of the DMCs provide an interesting physical conundrum, the question of how the species found to be in such a harsh environment such as the ISM posed a difficult one, which increased in depth with the discovery, during the 1960s, of yet more complex molecules such as Hydroxyl (OH), Ammonia (NH_3) and Water (H_2O). The problem with the existence of such diatomic and polytomic molecules is a question of energetics, one which will be discussed in depth later.

Snow & McCall (2006) characterise DMCs in four different sub-classes, a summary of which can be seen in *Table 1.2*. The parameters defined within the table reflect the attributes of the local environment of a parcel of gas rather than an average over the complete line of sight. This is so as to reflect the complexity of the ISM over the size scale that a DMC occupies. That is; the ISM can be, and often is, regarded as a discrete areas of type; Cold Neutral Medium, Warm Ionised Medium and the Hot Ionised Medium (sometimes referred to as the inter-cloud medium).

	Diffuse Atomic Cloud *(DAC)*	Diffuse Molecular Cloud *(DMC)*	Translucent Cloud *(TC)*
Molecular Classification	$f_n(H_2)<0.1$	$f_n(H_2)>0.1$, $f_n(CO)<0.9$	$f_n(C^+)<0.5$, $f_n(CO)<0.9$
A_v (min)	0	$\sim$0.2	$\sim 1 \rightarrow 2$
Typical n_{H_2} (cm^{-3})	$10 \rightarrow 100$	$100 \rightarrow 500$	$500 \rightarrow 5000$
Observational Techniques	Optical, 21cm	Optical absorption, mm absorption spectra	Optical absorption mm absorption and emission

Table 1.2: Physical Attributes of Diffuse Galactic Clouds
Table data adapted from Snow & McCall (2006)

It is important to recognise that in addition to the gas-phase species within the cloud, there exists grains of dust which account for approximately 1/100 of the cloud's mass. These dust grains, as is discussed later, contribute to the physics chemistry occurring in the cloud through the reactions taking place on the dust-grain surfaces, absorption and re-emission of background photons and attenuation of radiation. As can be observed in the table above, the UV and and visual spectrum are used in observing the diffuse clouds, therefore consideration of the extinction caused but the habituating grains are important in determining the cloud's chemical dynamics. Returning to consideration of *Table 1.2*; the additional sub-categorisation of the Diffuse Atomic Clouds (DACs) allows for a more complete description of the cloud's state. However previous works, such as Burgh et al. (2007), classifies only two forms of diffuse media, those being; the diffuse and translucent regimes with the limit being $Z(\frac{CO}{H_2}) < 0.25$ and $\frac{A_v}{d} < 1$ mag kpc^{-1}, which is similar to the limits stated above.

1.1.1 Diffuse Atomic Clouds

DACs are are where Diffuse Interstellar Band Carriers (DiBs) populate. DiBs are give rise to unidentified features in the spectra of background objects, these were first noticed around 80 years ago by Heger (1922). She noticed a set of stationary features at the 5780Å and 5797Å lines of a spectroscopic binary system. The description was coined due to "diffuse"; because the spectral absorption lines were broader than the accepted molecular lines, "interstellar"; because it was thought that these lines' source was in the medium between stars. Though initially some thought that the source of these lines were in fact molecules residing in the ISM (eg, Russell (1935); Swings (1937); Swings & Rosenfeld (1937)), the lack of understanding as to the existence of gas-phase molecules and their respective reactions with

one another caused the emergence of a solid state solution to the problem. With the advent of more sensitive observation equiptment in the 1960s, the detection of ISM molecules at radio wavelengths became possible (Weinreb et al. (1963)) and hence a molecular gas-phase solution was defined through the ion-neutral interaction (see later). DiB traces are found to be within the spectra of reddened stars, they generally correlate well with A_v, however for high A_v it levels off, implying that residence within DACs. The present thoughts for the causes of these lines are large, organic, gas-phase molecule interactions within the clouds.

The DACs are exposed to the harsh radiation field in the ISM, therefore almost all of the constituent molecules are photodissociated, resulting in a highly sparse environment. The cloud mainly consists of atomic Hydrogen, atoms with ionisation potentials less than that of Hydrogen are found to be in their ionic forms, which provide an abundance of electrons within the cloud. The main tracer of the DACs is the 21cm HI line,Dickey & Lockman (1990) .The scarcity of molecular matter in implies a lack of chemistry occurring in the DAC but, as we have seen, the mere implied presence of the DiBs within these structures causes one to question our understanding.

1.1.2 Diffuse Molecular and Translucent Clouds

Unlike the DACs, DMCs reside in areas where the interstellar radiation field has been attenuated at wavelength(λ_{att}) to a degree where the photodissociation of Hydrogen no longer occurs, due to the effect of shelf sheilding, Snow & McCall (2006). This phenomena is reflected in the substantially higher Hydrogen fraction detailed in *Table 1.2.* However, note that the radiation is still sufficient, at $\lambda \neq \lambda_{att}$ photodissociation of CO still occurs thus Carbon still remains in its ionised form. The attenuation of the ISM radiation is provided by an envelope of atomic gas surrounding the DMC, this protection allows gas-phase molecule reactions to occur, either through ion-neutral reactions or by dust-grain adherence (both of which are discussed later). The product of these reactions are detected in the absorption spectra of the clouds, the main observational bands are the Optical (CO, CH, CN, C_2C_3), the Infra-red (CO, H_2^{3+}) and at λ_{mm} (HCO^+, OH, C_2H). Finally it is important to note that since the DMC are surrounded by an envelope of atomic gas, that any line-of-sight measurement will include a certain level of the atomic component, this will yield a Hydrogen fraction significantly lower than the fraction at the cloud's core.

If one were to increase the level of attenuation of the radiation incident on the cloud, one would 'create' a TC. The increased attenuation of radiation in the TC regime allows for the cessation of the photodissociation of Carbon which, in turn, allows the transcendence of C^+ to its molecular form (CO). Chemical reactions in the TC differ significantly from the DMC regime, the reduction in the number of electrons and an increase in the number of C^+ ions, this transition was first observed by van Dishoeck and Black1989. The TC must

be surrounded by molecular material to be in a steady state, the existence of these TCs where $A_v < 1$ is thought to be impossible. It is therefore plausible that if one considers a time, t_0 where a parcel of gas exisits in the ISM before interaction with the ISM radiation field occurs. As time progress from $t_0 \rightarrow t_0 + \delta t$, as δt increases it would be possible to track a pseudo-evolutionary track along these cloud types from DAC $\rightarrow$ DMC $\rightarrow$ TC, since each cloud type requires the presence of its predecessor to exist. In total, Diffuse Clouds represent a small fraction of the overall cloud structure and gas content of the Galaxy and are never sources of star formation, McKee (1989); Blitz & Williams (1999); Stahler & Palla (2004).

1.2 Giant Molecular Clouds

Giant Molecular Clouds (GMCs), present a completely different dynamical chemical environment than the cloud types previous discussed. A GMC is an aggregation of atomic HI and molecular H_2 gas clouds, some believe, which can exist for prolonged lengths of time through a equipartition of pressures, Stahler & Palla (2004). Though others, such as Elmegreen (1990a); Elmegreen (1990b); Ballesteros-Paredes et al. (1999); Klessen et al. (2004) and Ballesteros-Paredes (2006) believe that GMC formation is a *less harmonious* process which is due to random collisions, gravitational instabilities and turbulent motions due to turbulent initial conditions (Glover & Mac Low (2007)). The thermal motion of the cold gas core is regulated by the warmer, more diffuse, envelope (similar to the DMCs). This environment leads to a situation in which star formation can commence, this occurs through the gravitational condensation of matter into areas of more dense gas. GMCs are essentially a compound structure which are created through the aggregation of smaller *clumps* of gas into a larger structure, similar to Galaxies leading to Groups which can lead to Clusters and so on. Though it is better to think of the GMC as an area of continuous gas where the clumps are areas of relatively high density than when compared to the inter-clump medium, Evans et al. (1999); Snow & McCall (2006).

From observation, Stahler & Palla (2004), it is possible to deduce that the clustering (hence forming the GMC) occurs as gas flows into potential wells along the spiral arms of the Galaxy. Molecular clumps form within the GMC through condensation, this is a self protecting process by which the condensation of atomic to molecular matter leads to shielding from the UV radiation causing the photodissociation of the products which, in turn, assist in the production more more molecular matter. The space between *clumps* is occupied by the ICM which is of lower density, as previously mentioned, than that of the clumps. Through the detection of $^{13}C^{16}O$ absorption lines, it is possible to deduce that some fraction of the ICM is molecular, with the remainder being atomic in nature, detected through the 21-cm line. The atomic gas envelopes of the GMCs, in linear size, are significantly larger than the

complexes which they surround. On average a GMC envelope can extend for several times the linear size of the cloud, Weinreb et al. (1963); .

1.2.1 GMC Support

It is still a controversial matter as to whether the individual velocity dispersions of clumps within a cloud is random with no systematically significant motion to a common point of collapse. If this were true then it would imply that a GMC complex structure is in equilibrium until destroyed by the stars which it spawns. However, it is commonly thought that the clouds are in equipartition of the thermal, kinetic, gravitational and magnetic pressures. It is this *balance* of these pressure which maintain the GMC structure. Using the Virial Theorem, one may assume that a balanced cloud may be in a state of Virial Equilibrium, or Energy-Equipartition (Ballesteros-Paredes (2006)), hence the following can be considered to be true;

$$2T + 2U + W + M = 0 \tag{1.1}$$

Where T is the total kinetic energy of the bulk motion, U is the energy contained in the random thermal motion, W is the gravitational potential energy and M is the energy associated with the magnetic field. Though the equation appears to be showing all the pressures/energies are equatable to one-another. This is an incorrect assumption. Consider, instead, a spheroidal shell encompassing the 'complete' cloud, this equation describes the equipartition of net flow of energy through the surface of the shell. For the expressions for each of the parameters see Stahler & Palla (2004). The expression gives the impression that the clouds are somewhat docile and in equilibrium. However, other authors such as; Blitz & Shu (1980), Ballesteros-Paredes et al. (1999), Elmegreen (2000), Ballesteros-Paredes (2006) and Ballesteros-Paredes et al. (2008) believe the clouds to be more dynamic and energetic than transient. With the clouds having short formation times, and having a rapid evolutionary sequence due to the high velocity HI streams within the cloud causing disruption and density fluctuations within the cloud complex. (Ballesteros-Paredes et al. (1999)). Also, the equilibriate and virial consideration of the clouds' nature and in description of their formation and existence is questioned, Ballesteros-Paredes (2006). The internal magnetic field of the complex is estimated by the Zeeman splitting of the OH and 21-cm spectra lines (see later), it is noted that the internal magnetic field of the complex acts orthogonally to that of the $|\mathbf{B}|$ in the Galactic plane. The direction of the interior magnetic field is determined through the measurement of the polarisation of background light as it passes through the GMC complex. Any well ordered field in a self-gravitating cloud would cause matter to stream along the field lines until a planar structure for the complex is reached. Planar flattening does not appear to occur through the current observations of GMC and hence the interior field is thought to be smooth in nature. Internal field distortion arises from Magnetohydrodynamic waves, these MHD waves assist in the prevention of flattening of the

GMC, Stahler & Palla (2004). The main source of complex support arises from the internal kinetic energy of the component clumps, which are determined through the broadening of the CO spectral line.

1.2.2 Star Formation : The Death of a Cloud

Star formation occurs through the gravitational condensation of matter within a cloud into areas of, eventually, significantly higher density. Local over densities in the GMC cause minor fluctuations in the gravitational potential of the cloud, which cause minor potential wells. These potential wells allows the flow of gas into them, thus increasing the local density, which increases the potential and hence attracts more matter. GMCs tend to produce OB associations which are the source of the cloud's destruction. The stellar winds produced by the young stellar populations and the association heating of the cloud causes the atomic and molecular surrounding gas to disperse. As the GMC grows older the internal structure evolves into having smaller *clumps* of smaller diameter and larger *bubbles*, i.e. the more dense regions reduce hence increasing the areas of lower density through the creation of stellar populations. An example of this is the gravoturbulent fragmentation of the molecular cloud, Klessen et al. (2004). This where the stellar clusters form through the supersonic turbulence within the gas which is constituent to the cloud. It is the turbulence which causes the fluctuations in density, this is exacerbated in areas of higher density thus promoting local collapse through gravitational instability in these areas. This leads to the formation of stellar material, hence stars leading eventually to stellar clusters.

1.3 Dark Clouds

Dark Clouds represent the coolest and most dense regions of the ISM, Bergin & Tafalla (2007). This species of Galactic Molecular Cloud falls into two distinct classifications. Referring to table 1.1, there are individual and complex systems of dark cloud. Stahler & Palla (2004) state that the clumps within the GMCs are essentially individual Dark Clouds, the largest of these clumps have been found to be of the order $10^3 M_\odot$. However, larger Dark Clouds, of similar density but with mass of order $10^4 M_\odot$ exsist and are referred to as Dark Cloud Complexes (DCCs). Dark clouds are named such due to their high column densities ($n_{H_{2_{peak}}} \geq 10^{23} cm^{-2}$) and opacities ($A_{v_{peak}} = 100$), Du & Yang (2008); van der Wiel & Shipman (2008). This causes the Dark Clouds to appear as dark extinctive features on an otherwise radiatively bright background.

1.3.1 Dark Cloud Complexes

Dark Cloud Complexes account for a significant fraction of star formation in galactic clouds, however, unlike previous cloud types the DCCs do not form OB associations (usually synonymous with larger, more massive, stellar formation systems)The most commonly studied for of DCC are the infra-red incarnation of the type. Since the extinction of infra-red radiation is significantly lower than that for the optical regime, the distances to which the IRDCCs can be observed is larger hence a lager sample of data is available. With this observational data being more readily available for the IR regime the comprehensive sky coverage mainly due to large area IR surveys such as 2MASS, Skrutskie et al. (2006), and the *Spitzer Space Telescope*'s Galactic Legacy Infra-red Mid-plane Survey Extraordinaire (GLIMPSE; Benjamin et al. (2003)) extinction mapping has begun to combine the number density of stars with the associated colour information (Cambrésy et al. (2002)). Typical size and mass scales for the IRDCCs are $\sim 5pc$ and $10^3 - 10^4 M_{\odot}$. The temperature of emission for the complexes is $\sim 25K$ causing them to generally emit at $8.6 \rightarrow 10.6\mu m$.This low temperature implies there is a lack of massive star formation which is usually associated with the more dense cloud morphologies, conversely; the conditions described make them exemplary candidates for the sites of early stages of star formation, Simon et al. (2006).

The earliest investigations into optically thick, so called, "Dark Regions", "Dark Nebulae" or "Dark Clouds" were conducted by; Barnard (1919a); Barnard (1919b); Bok & Reilly (1947); Lynds (1962) and later by Feitzinger & Stuewe (1984). However, many of the IRDCs were omitted from the final catalogues because the searching for these clouds was conducted by eye and hence many remained excluded from the data. The IRDCC subclass were discovered by the Midcourse Space Experiment (MSX), Egan et al (1998), as dark foreground extinctive features on the otherwise radiatively mid-infrared background. The shape of the DCCs can be either compact (core-like) or filamentary in nature (similar in morphology to that of galaxy cluster aggregations). It has been found, through observation of the clouds, that the distribution of the IRDCCs peaks towards sites of star formation, the spiral arm tangents and the $5kpc$ Galactic molecular ring. Though Du & Yang (2008) suggests this distribution may be nothing more than an amplified selection effect and states a larger, more uniform survey, would be required to ascertain whether this pattern is true . van der Wiel & Shipman (2008) states that; it has not yet been established whether, or not, all IRDCs harbour active star formation or just starless cores. Though work by Bergin & Tafalla (2007) suggests that the Dark Clouds represent the most accessible sites where solar mass stars can be born.

Though research into the nature (and possible nurture) of the DCCs is ongoing, several questions remain unanswered; Is there an evolutionary path within the DCC class? Are DCCs part of some larger evolutionary sequence, of which we only have a snap-shot? Some

schools of thought believe that the DCCs are in fact evolutionary stepping stones, an intermediate species, linking the GMCs with the Dense Cores (and Bok Globules), and that there is a, currently misunderstood, mechanism linking all three cloud classes. Du & Yang (2008) goes on to state that we may only truely understand the links, if any, between these classes via more detailed mapping of the sources using a variety of tracers, only then may these issues be clarified.

1.4 Dense Molecular Clouds

The final cloud type to be discussed here is the Dense Molecular Cloud (DMC). Within this section there are two sub-classes of this cloud; the Dense Cores are dense compact DMCs which reside within some larger molecular complex structure, the second is the Bok Globule; named for the astronomer whom first observed these objects. The extrinsic difference between the Dense Cores (DCs) and the Bok Globules (BGs) is; where the DCs are embedded in a larger cloud structure, the BGs are not. So BGs may be considered as isolated cores, giving information that would otherwise be unavailable in an embedded core observation, Stahler & Palla (2004).

1.4.1 Dense Cores

The molecular line characteristics of these cores will not be discussed in detail here, however, for completeness it is noted that the different molecular line transitions require varying levels of hydrogen density, n_{H_2}, to allow the transition excitation to occur.

DCs which have not yet formed stars are said to be pre-steller or starless cores, these are considered to be the earliest form of this cloud-type. These pre-stellar cores are characterised by a distinct lack of any point IR source at the centre of the cloud, Tafalla (2008), though this could be due to current limits in millimeter and sub-millimeter sensitivity and resolution. Starless cores tend to reflect a somewhat uniform density of $10^5 \rightarrow 10^6 \mathrm{cm}^{-3}$ for the central region, R $< 5000 \rightarrow 10000$ AU. Outside this central area, the density drops off as a power law at larger distances.

As the Dense Cores evolve; self-gravitational collapse through local fluctuations in the distribution of matter causes an increase in the central point density. Eventually this over density will reach a limit where, the point density causes gravitational instability in the core, Tafalla (2008). This gravitational instability causes the core to condense and collapse; DCs are sites of major star formation, the condensation, through rotational collapse, of the DC matter forms stars. This collapse causes the magnetic field lines interior to the core to become parallel to the gas motion. This occurs to a set limit where the magnetic pressure generated by the compression of field lines equals that of the self-gravitating, which impedes

any further collapse. This amplifies any initial rotational motion through conservation of angular momentum. A rotating, dense, core of mass M, diameter L and angular velocity ω, the rotational kinetic energy, τ_{rot};

$$\tau_{rot} = \frac{1}{20} M L \omega^2 \tag{1.2}$$

It is possible to equate this rotational energy to that of the gravitational potential energy generated by the core;

$$\frac{\tau_{rot}}{|W|} = \frac{\omega^3 L^3}{24GM} \equiv 10^{-3} (\frac{\omega}{1 kms^{-1} pc^{-1}})^3 (\frac{L}{0.1pc})^3 (\frac{M}{10 M_\odot})^{-1} \tag{1.3}$$

Equation 1.3 implies that the DCs rotate slowly with period; $\frac{2\pi}{\omega} \sim 6 \times 10^6$ years. Notice rotation period, it is of the order of the actual cloud lifetime ($\sim$10 Myr; Blitz & Shu (1980)), this is where authors such as Stahler & Palla (2004) establish that the molecular clouds are somewhat quiescent in nature. Since the observable dynamics change on a comparable time-scale to its lifetime.

Shifting our attention from the embedded cores to that of, the previously mentioned, Bok Globules (BGs). With the exception of their relative isolation exterior to larger cloud complexes, the BGs are essentially the same, in physical attributes, to that of the embedded DCs. Their sparse surroundings and simple appearance make BGs ideal candidates for high resolution mapping of DCs. BGs tend to consist of a core, mass of the order $10 M_\odot$, which is then surrounded by an envelope of gas approximately twice the mass of the BG-core. At the centre of the BG, so far only IR stars of low luminosity have been detected. A typical example of this is object *object 5335*, near the peak density of its core, lies a far infra-red star of luminosity $3 L_\odot$, Stahler & Palla (2004). Thus far, research into BGs have only yielded detections of low IR luminosity stars at the centre of BGs and DCs alike.

This forces one to postulate on where more massive stars are formed. How, for example, are massive stars formed if, even in the most dense regions, stars of relatively low luminosity/mass are *born*? BGs could be the solution to this problem. One may consider BGs to be the remnants of such a birth, the cores of once large cloud complexes which have long been dispersed by both radiative and stellar pressure or the formed stars it once contained, Stahler & Palla (2004); Simon et al. (2006). However, this is difficult to observe directly; since high mass stars tend to disperse their parent clouds over a time scale significantly shorter than that of the stellar lifetime, it is difficult to observe the birth of such O and B stars, but relatively easy to observe the destructive consequences.

Chapter 2

Chemical and Physical Processes within Molecular Clouds

Within even the most quiescent clouds, there exists some degree of dynamical perturbation due to the processes occurring in the cloud's interior. Most reactions tend to be occur when an ion interacts with a stable molecular form thorough the slight polarisation of the neutral atom, causing an instantaneous-induced dipole electrostatic attraction.

$$\alpha^{\pm} + \beta \rightarrow \gamma^{\pm} + \delta \tag{2.1}$$

Note : if $\alpha = \delta$ and $\beta = \gamma$ then the reaction is merely *Charge Exchange*

The ion-molecule reaction pathway allows reactions within even the coolest clouds, in which the temperature is too low for the neutral-neutral reaction pathway to overcome its associated potential barrier ($\frac{\delta E}{k_b} = 1000K$). During the early 1970s (Stahler & Palla (2004)), the ion-molecule pathway has been accepted as a possible route to overcome the potential barrier. It was found that the effective cross-section of the reaction, due to the long-range nature of the electrostatic attractive force, was greatly increased when compared to that of the cross-section of a solely collisional reaction mechanism. Even at Dark and Dense Cloud temperatures, the reactions can proceed with enough pace to account for the observed abundances of the isotopologues for various species.

Though the expression in equation 2.1 shows that reactions involving negative ions are possible, they are less frequent that those involving a positive speicies. The only difference with negative reactions are that there is a free electron as one of the products. The free electrons created by negative-ion interaction destroys the positive ionic species in the clouds. Often, auto-ionisaton occurs with the species just re-emitting the electron into the intra-cloud medium. However, if the reacting species spits before auto ionisation occurs;

$$\alpha^+ + \mathrm{e}^- \rightarrow \beta + \gamma \tag{2.2}$$

Thus, two neutral molecules will be the product of the reaction. Most of the processes detailed in this chapter occur via the reaction mechanisms above. The exception being H_2 which forms using the surface of the clouds dust grains as a catalyst surface on which to adhere.

2.1 Grain Surface Adheretion and Catalysis

The mechanisms detailed in equations 2.1 and 2.2 are, as with terrestrial reactions, governed by the reaction rate which in turn is governed by the reaction conditions and concentrations of the reactants. The ion-molecule reaction pathway does not account for the formation of all the molecular species in the intra-cloud medium. In addition to direct chemical and physical reaction for the depletion and creation of species, one must consider how the molecular and atomic matter interacts with the granular dust, a consideration more applicable to that of the denser cloud forms.

Considering a cloud of volume, V with a number density of dust grains, n_d each with a cross-sectional area of πa_d^2 and a thermal velocity of V_{therm}. Hence the probability of a molecule sticking to the grain is the ratio of the total volume of the cloud to $n_d \pi a_d^2 V_{therm}$. Inversion of this probability yields the average time per collision, t_{coll};

$$t_{coll} = \frac{1}{n_d \pi a_d^2 V_{therm}} \tag{2.3}$$

Since $t_{coll} <<$ cloud lifetime (of the order 10^6yrs, Blitz & Shu (1980)), it leads one to assume that there is a mechanism that re-injects the adhered matter back to the gas-phase (desorption). Bergin et al. (1995), suggests that this desorption occurs due to four possible mechanisms; thermal evaporation, cosmic-ray interaction and direct-photon absorption (as postulated by Stahler & Palla (2004)). Heating through cosmic-ray interaction has been found to be an effective adsorption mechanism, one that operates throughout the cloud's core, Willacy & Williams (1993). Where as the photon desorption through the interaction of UV photons has been found to be somewhat unimportant, due to the density of the cloud causing absorption of the incident photons, D'Hendecourt et al. (1985). The final method by which molecules are returned to the gas-phase is through grain-grain collisions, though the grain-velocities required to achieve such a reaction is greater than the thermal velocity for the cloud, D'Hendecourt et al. (1982). Little information is known with regard to dust grain velocities within clouds, making it difficult to assess the contribution of this effect to the overall desorption rate. The desorption rate for a given cloud is a cumulative effect over all the different mechanisms rather than discrete rates per type, Bergin et al.

(1995). In addition to adsorption and desoprtion, the dust grains provide a reaction surface by which molecules which could otherwise not be formed are generated before desorption. An example of such a molecule is H_2, Cazaux & Tielens (2002).

2.1.1 Formation of H_2 through Dust Grain Catalysis

This section is concentrates on the physical mechanism of the reaction rather than the involved chemistry, this is discussed later. In symmetrical molecules (lacking a dipole moment), such as H_2, even the lowest allowed energy levels have a significant potential barrier to overcome to allow population. The lowest excited energy states are rotational, these rotationally excited molecules radiate slowly within the ground state. The allowed transitions are significantly slow enough that the collisional reaction of two free independent atomic species does not result in a molecular product. The presence of the dust grain allows for a third party to absorb the emitted energy to allow this slow transition to take place.

Consider two Hydrogen atoms, H_α and H_β; The first incident atom, H_α, is attracted to the dust grain by a van der Waals attraction and adsorbs to the dust's surface. So as to exist at the lowest possible energy, H_α quantum mechanically tunnels to find a defect in the structural lattice. Once at this defect, the H_α atom forms a stronger bond with the structure using its unpaired electron. The difference in binding energy strength between the van der Waals and the ionic lattice bond is; $\frac{E_{IB}}{E_{vdW}} = 2.5$. Within a time interval, given by t_{coll} (equation 2.3), a second atom, H_β, attracted to H_α, finds a binding site near to H_α and the two atoms combine. Post-combination the molecular hydrogen created does not have an unpaired set of electrons and is therefore only weakly bonded to the granular surface, hence, through the mechanisms stated above, the H_2 returns to the gas-phase. However, some aregue that a cloud lifetime of 1-2 Myr is too short to account for the formation of the *required* volume of H_2. A approximate H_2 formation rate is described in Hollenbach & Salpeter (1971);

$$\mathrm{t_{formation}} \simeq \frac{10^9 \mathrm{yr}}{\mathrm{n}} \tag{2.4}$$

Where n is the number density in cm^{-3}, suggesting, for a cloud averaged density of $\overline{n}$ $\sim$100cm^{-3} conversion of atomic to molecular Hydrogen takes longer than the lifetime of a transient cloud; approximately 10 Myr, Blitz & Shu (1980). This approximation, however, does not take into account turbulent conditions within the clouds, Glover & Mac Low (2007).

2.2 The Molecular Constituents of Clouds

So far we have discussed the various classification of clouds by physical appearance and also the possible reaction mechanisms within. Now we move onto the main constituent molecules of these clouds, how they are produced, which isotopologues are and how each of these isomers are detected and what information that imparts to the observer. Table 2.1 presents a list of useful molecules and their associated parameters. This is a much more comprehensive list than is required, hence this work will concentrate on Hydrogen (molecular and atomic), Carbon Monoxide, Hydroxyl and Ammonia. Since the formation of molecular hydrogen has been touched upon in section 2.1.1, we begin with the discussion of Hydrogen.

Molecule	Relative Abundance	Transition Type	Detected λ	T_0 (K)	n_{crit} cm^{-3}	A_{ul} (S^{-1})	Tracer of
H_2	1	vibrational	2.1μm	6600	$7.8x10^{7}$	$8.5x10^{-7}$	Shock
CO	$8x10^{-5}$	rotational	2.6 mm	5.5	$3.0x10^{3}$	$7.5x10^{-8}$	Low Density
OH	$3x10^{-7}$	Λ-doubling	18cm	0.08	$1.4x10^{0}$	$7.2x10^{-11}$	Magnetic Field
NH_3	$2x10^{-8}$	inversion	1.3cm	1.1	$1.9x10^{4}$	$1.7x10^{-7}$	Temperature
H_2CO	$2x10^{-8}$	rotational	2.1mm	6.9	$1.3x10^{6}$	$5.3x10^{-5}$	High Density
CS	$1x10^{-8}$	rotational	3.1mm	4.6	$4.2x10^{5}$	$1.7x10^{-5}$	High Density
HCO^+	$8x10^{-9}$	rotational	3.4mm	4.3	$1.3x10^{5}$	$5.5x10^{-5}$	Ionisation
H_2O	$7x10^{-8}$	rotational	1.3cm	1.1	$1.4x10^{3}$	$1.9x10^{-9}$	Maser
H_2O	$7x10^{-8}$	rotational	527μm	27.3	$1.7x10^{7}$	$3.5x10^{-3}$	Warm Gas Probe

Table 2.1: Main Constituents of Galactic Molecular Clouds

T_0, equivalent temperature; n_{crit}, critical density of the main isotopologue; A_{ul} , probability per time of spontaneous decay from upper $\rightarrow$ lower state. Data adapted from Stahler & Palla (2004)

2.2.1 Hydrogen

The diatomic form of Hydrogen was first discovered in the interstellar environment in 1970. It was detected through rocket observations of several absorption lines, through photo-excitation of its electronic states, in the direction of O-type star ξ-Persei, Stahler & Palla (2004). Hydrogen is the main constituent of cold clouds, however it is also the most difficult to detect due to the lack of a dipole moment. The rotational levels of H_2 lowest decay is the J=2$\rightarrow$0 transition, this corresponds to emitted photon of wavelength; $\lambda = 28.2\mu m$. This line resides in the far-infra red and can only be detected through observations above the Earth's atmosphere. Whereas the 1-0 S(1) rovibrational line is detected using the 2.1μm

line.

In addition to the reaction on dust grain surfaces mentioned previously, it is possible for H_2 to form in an environment completely devoid of dust. However, this is only the case is the density and temperature of the local environment are high enough and providing the gas in which the Hydrogen resides is ionised. In these conditions two reaction coupled pathways are present;

$$H + e^- \rightarrow H^- + h\nu \Rightarrow H^- + H \rightarrow H_2 + e^- \tag{2.5}$$

Where $h\nu$ denotes a photon. The ambient photons created allow the production of H_2 through;

$$H + H^+ \rightarrow H_2^+ + h\nu \Rightarrow H_2^+ + H \rightarrow H_2 + H^+ \tag{2.6}$$

The above reactions are valid for the early Universe, before the condensation of dust, due to the limited supply of free ions the number of molecules created by this path would be small. It is noteworthy, however, that at sufficiently high temperatures the following reaction takes place;

$$H + H + H \rightarrow H_2 + H \Rightarrow H_2 + H + H \rightarrow 2H_2 \tag{2.7}$$

Which, according to Stahler & Palla (2004), could have formed the first molecular clouds. The depletion of H_2 occurs via the photodisociation of the molecule by UV photons produced by O and B type stars. Because of this photodisociation, it is not possible for there to exist a cloud of pure molecular Hydrogen. H_2 becomes self-shielding through the creation of an atomic envelope around the H_2, which protects the interior Hydrogen from the photodiscociatative effect of the photons by cutting down the penetrating radiation.

2.2.2 Carbon Monoxide

Carbon Monoxide is the next most abundant compound after Hydrogen. CO, is created through gas-phase reactions, the species has a comparatively high binding energy (11.1 eV) thus protecting it from additional destructive reactions. Due to the self-shielding effect of CO, it aggregates in a similar manner to that of H_2 (but remains disociated to a greater depth), hence it allows CO to be an accurate tracer of the Hydrogen mass of the cloud.

One possible pathway of CO formation is through gas-phase reactions involving CH^+, CH and OH; (Oppenheimer & Dalgarno (1975); van Dishoeck & Black (1988)).

$$CH^+ + O \rightarrow CO + H^+ \rightarrow CO^+ + H \tag{2.8}$$

$$CO^+ + H \rightarrow CO + H^+ \tag{2.9}$$

$$CH + O \rightarrow CO + H \tag{2.10}$$

Unlike H_2, CO *does* have a permanent dipole moment which causes strong emission through the radio frequencies. CO is considered to be the primary tracer of molecular gas in both intra and extra galactic astronomy. The isotopologue which is easiest to detect, according to Stahler & Palla (2004) is $^{12}C^{16}O$, with $^{13}C^{16}O$, $^{12}C^{18}O$ and $^{12}C^{17}O$ proving useful. However, Goldsmith et al. (1997) state that $^{12}C^{18}O$ because $^{12}C^{18}O$ is not as susceptible to the optical depth problems associated with $^{12}C^{16}O$ and $^{13}C^{16}O$. The low critical density of CO allows it to be used to probe the lower density regions of clouds rather than dense cores. The reason for this being that within the cores themselves, the radiation of the detectable J= 1→ 0 transition is completely absorbed by optically thick core medium. It is for this reason that the other CO isomers are used since they are not optically thick in these regions. The CO is excited to the J=1 state by the collisional excitation of CO with H_2. The consequence of the collision is dependent on the ambient density of the medium. If the CO-H_2 collision occurs in an area of low ambient density, then the transition of the CO, J= 0→ 1 is immediately followed by the emission of a photon, resulting from the CO not having any other molecules with whom to transfer its energy . When the ambient density is high, then the CO can pass its energy to a H_2 molecule, which results in no photon emission, Stahler & Palla (2004). The lowest rotational levels of the CO energies and progressively occupied as the cloud density increases.

CO, in some more dense regions, also suffers from depletion through *Gas-Phase Freeze-Out*, Bergin & Tafalla (2007). This is where the CO molecules freeze onto the surfaces of the dust grains within the cloud itself. Thus removing that molecule from the gas phase and hence from being a possible reactant. This was found to dominate in clouds with densities higher than $\sim 3\text{x}10^{-4}\text{cm}^{-3}$, Bacmann et al. (2002).

2.3 Applications of Molecular Transitions

Generally speaking, to investigate and measure various parameters of molecular clouds. This section approaches each of the interesting features of the clouds and discusses which molecules are used to obtain information, how it is observed and which transition is used to observe it.

2.3.1 Mass - Approximation

Generally the mass of Hydrogen in a cloud approximates (to a statistically significant degree) the total mass of a galactic molecular cloud. However, as mentioned in §2.2.1, the symmetrical nature of H_2 causes it to lack a dipole moment and hence makes it very difficult to detect. To bypass this issue, research into how other molecular species behave and build

up discovered that the CO molecule amasses in a similar way to that of H_2 and hence if one can measure the abundance of CO one may infer the mass of H_2 and hence the entire cloud, Keres et al. (2003a);Keres et al. (2003b).

The transition of atomic to molecular Hydrogen occurs through self-shielding, forming an ionised atomic outer envelope which protects the H_2 in the centre, Hollenbach et al. (1971); Dickman (1978); Myers et al. (1986) causing molecular Hydrogen to build up in the interior. However, the transition of atomic to molecular Hydrogen facilitates the production of CO, not through dust-grain surface catalysis but through gas-phase ion-neutral reactions. The species, CII can react with either atomic or molecular Hydrogen and can react quickly with both;

$$C^+ + H_2 \rightarrow CH_2^+ \tag{2.11}$$

$$CH_2^+ + e^- \rightarrow CH + H \tag{2.12}$$

$$CH + O \rightarrow CO + H \tag{2.13}$$

An important feature of the Carbon involved here is that the first ionisation potential is equal to that of the Lyman-α excitation energy (11.6eV). This means that photons of this energy are quickly depleted by the *atomic* Hydrogen and the CII through the reactions above, this causes the build-up of *molecular* Hydrogen and CO. Hence the determination of the amount of CO within a cloud gives information as to the molecular Hydrogen content and thus the mass, Oppenheimer & Dalgarno (1975); Leisawitz et al. (1989); Stahler & Palla (2004); Burgh et al. (2007) . For completeness; the presence of carbon is not always in compound form throughout the cloud. The gas-phase Carbon is converted from CII $\rightarrow$ CI $\rightarrow$ CO as one progresses to greater depth within the cloud.

As mentioned above, in the previous section, the J(1$\rightarrow$0) transition is used to measure the abundance of CO. There are many isotopologues of CO, the choice of which isotope to use depends on the optical thickness of the isotope in the region one is interested in. Any determination of mass must begin with the determination of the column density for a given molecule, the ease of which is heavily dependent on the optical thickness of of an isotope at a given frequency. If an isotope is optically thick at a given frequency then it absorbs the photons a frequency, ν_0 and for small $\pm\delta\nu$, which causes photons to be re-emitted to foreground observers. Each of the dynamic molecules have a line-of-sight velocity; this velocity, V_{los}, causes the re-emitted photon to be doppler shifted. This doppler-shifting causes the line emission profile to be broadened for observations of the molecule at, or near to, frequency ν_0. Therefore, emission is only detected from the surface of the cloud.
Conversely, if an isotope is optically thin for observations centred on ν_0; the detected flux can be considered to be incident from all points of depth within the cloud. This can be

considered to be representative of the total emission along the entire line of sight from within the cloud. In this condition, the observed amplitude for a given isotope intensity is reduced, when compared to the optically thick case, but is more sharply peaked at ν_0. Hence an integration of intensity over the frequency range is proportional to that of the isotope's column density. From this, it is now obvious why this proportionality cannot hold for the optically thick case because the radiation is radiated from the effective surface of the cloud, hence no information as to the interior is obtainable. The optically thin isotope for this transition is^{13}C^{16}O . Though the isotope ^{12}C^{18}O is optically thin, it is more difficult to detect and hence the former isotope is preferred,Stahler & Palla (2004).

Once the column density of the CO has been determined, one may begin to calculate the Hydrogen mass, this is generally inferred through a relationship between the column densities of the CO and Hydrogen. In any case, the abundance of CO must be proportional to the total Hydrogen adundance and not just the fraction of HI or H_2. Rather empirically, the column density of a given isotope is proportional to that of the optical thickness; from this Stahler & Palla (2004) determine;

$$N_{CO}^{13} = \frac{8\pi\Delta\nu_0^{13}Q^{13}\delta\tau_o^{13}}{c^2A_{10}}(\frac{g_0}{g_1})[1-\exp(-\frac{T_0^{13}}{T_{ex}^{13}})]^{-1} \tag{2.14}$$

Where; Q^{13} is the partition function, $\Delta\nu_0^{13}$ is the full width half maximum of the broadened line, T_0 is the equivalent temperature ($\frac{h\nu}{k}$) for the transition and T_{ex} is the excitation temperature.

From the above equation it is possible to derive a value for the column density of one's chosen isotope, in thie case ^{13}C. One may then seek to derive a relationship between the Hydrogen and Carbon Monoxide content of the studied cloud, the figure below (fig 2.1) presents a schematic view of this.

The empirical assumption of tis method, as detailed in Stahler & Palla (2004), is that the column densities of both Hydrogen and CO are linearly related, by some factor 'X'. One must choose a parameter to related the amounts of CO and H to which is observable in both the diffuse and the molecular regimes of cloud, generlaly the extintion values, A_v is selected. By equating N(CO) to A_v and N(H) to A_v one may infer a relationship between N(CO) and N(H). Firstly, the Hydrogen density may be determined through observation of the stars background to the cloud. The absorption of the cloud causes a dip in (B-V) space, which allows one to infer the a relation between NH) and the E(B-V) quantity and hence A_v. One may extend this treatment to include the molecular cloud class, providing the dust composition of the two cloud forms are not significantly different. The N(CO) is obtained through the measurement of the intensity of the CO spectral line (J(1→0)). The extinction may be estimated, providing the overall opacity of the cloud is low enough, by observing (figuratively) the background stars.Though the use of extinction maps is preferable in this

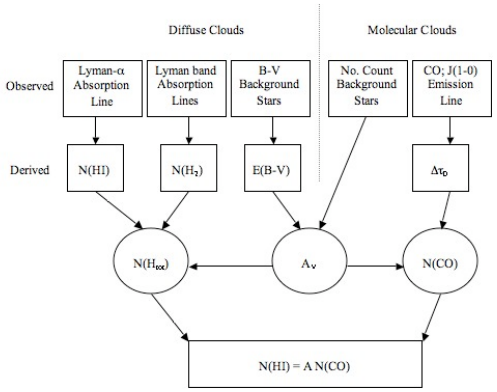

Figure 2.1: Steps by which one may derive the Hydrogen content of a molecular cloud, adapted from Stahler & Palla (2004)

case since it will yield a more accurate result.

If one assumes that the magnitude of a given star beyond the cloud, is reduced in apparent visual magnitude by Δm, in addition to this; any observation of said star will yield a distance greater than the actual position of the star. The star's distance, as a function of apparent magnitude excluding cloud extinction, is given by the relation;

$$\Delta log(r) = 0.2\Delta m \tag{2.15}$$

This holds for stars exterior to the cloud, for stars interior to the cloud there must be a deviation from linearity.
From this one may derive a relation between N(CO) and A_v and hence between N(CO) and N(H). By this method, Stahler & Palla (2004), state an uncertainty of 50% which one must account for via the determination of rarer CO isotopes and relating the new column density, though isotope abundance ratios, to that of N(CO) stated above. One must note that this method only holds true for galactic clouds and its high level of uncertainty questions its validity. However, a more precise method for intra- and extra-galactic clouds is the velocity integrated profile of from $^{13}C^{16}O$ and $^{12}C^{16}O$ emission. Which yields a result much lower in uncertainty.

2.3.2 Mass - Determination

The method previously detailed, as mentioned above, at best has a 50% uncertainty. Using the method detailed in Goldsmith et al. (1997); if one assumes that for a given transition, the emission is optically thin and that all the excitation temperatures are larger than the

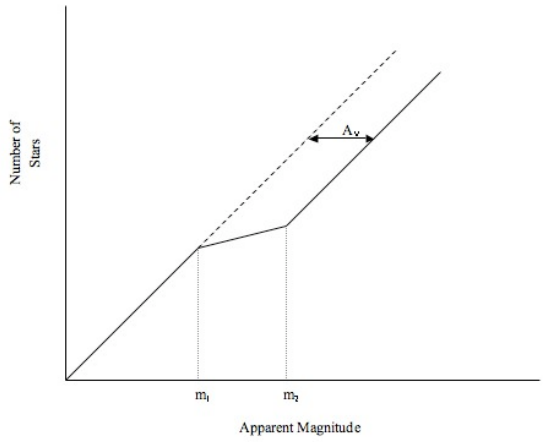

Figure 2.2: Determining A_v for a molecular cloud, adapted from Stahler & Palla (2004)

background temperature. The integrated temperature over the whole brightness directly gives information as to the column density of the upper level;

$$\mathrm{N_u(cm^{-2})} = \frac{8\pi 10^5 \mathrm{k}\nu^2}{\mathrm{A_{ul}hc^3}} \int \mathrm{T_{mb}d}\nu \tag{2.16}$$

Where; k is Boltzmann's constant, A_{ul} is the Einstein coefficient of spontaneous emission, ν is the frequency of emission, h is Planck's constant and c is the speed of light. T_{mb} is the main beam brightness temperature integrated between the frequency spread. This gives a parameter in units of K $\mathrm{kms^{-1}}$. This, however, only yields the column density of that of the upper energy states, there is a correction factor that must be employed to convert the obtained column density to that of the total molecular column density. This correction factor (CF) is expressed as the ratio of two sums;

$$\mathbf{CF} = \frac{\sum_{\mathrm{J=0}}^{\infty} \mathrm{N_j}}{\sum_{\mathrm{J_{u_{observed}}}} \mathrm{N_{J_u}}} \tag{2.17}$$

Where J_u is the upper level of each observed transition. Local Thermodynamic Equilibrium (LTE) is often assumed and then evaluation of the fraction of total column density that would be in the upper level in the transitions observed. In some cases, a non-LTE solutions may be used in which case Statistical Equilibrium is utilised to determine the column densities. The CF varies with molecular Hydrogen density, however, knowledge of the excitations are required for accurate calculation.

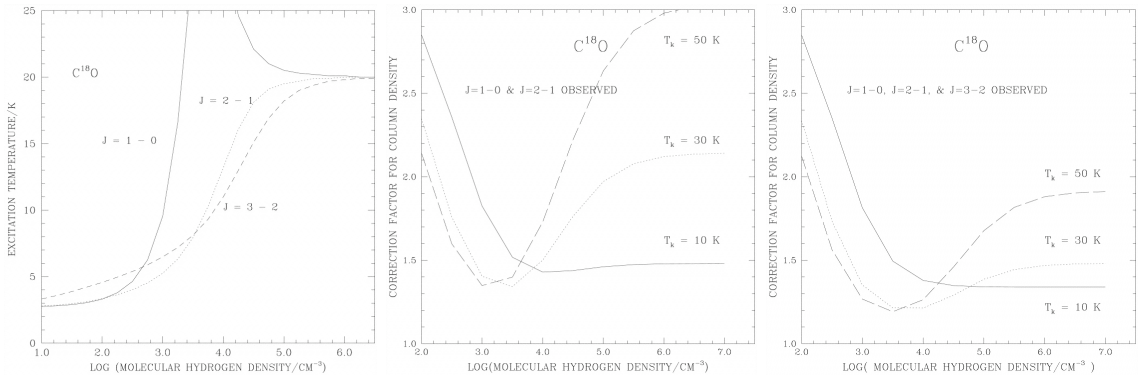

Figure 2.3: Correction Factor of the CO column density when the tow lowest transitions are observed. left; T_{kin} = 20K. Taken from Goldsmith et al. (1997)

Figure 2.3 shows that there is very little variation in the value of the CF over varying conditions; for $\log(n_{H_2})$ >3.5 there appears to be negligible dependence of CF on the Hydrogen density. However, from the figure it is obvious that there is a heavy dependence on the kinetic temperature of the cloud. Therefore, it is imperative that a temperature that best characterises the Carbon Monoixde along a given line of sight. Generally the kinetic temperature structure for a given cloud is traced by the distribution of CH_3CCH, as discussed in Bergin et al. (1994). though Stahler & Palla (2004) state that the inversion lines of NH_3 may also be utilised to this end. The kinetic temperature map is different for each cloud, therefore one must calculate the kinetic temperature individually.

2.3.3 Kinetic Temperature

For kinetic temperature, Stahler & Palla (2004) and Walmsley & Ungerechts (1983) state; the inverted spectral lines of Ammonia (NH_3) may be used to charaterise the kinetic temperature of a given cloud. This inversion arises from the oscillation of Nitrogen atoms through the Hydrogen plane. In a majority of molecules, vibrational transitions yield infra-red photons. The inversion transition of NH_3, in contrast, emit microwave photons. Classically this occurs because the Nitrogen atoms does not have sufficient energy to overcome the potential barrier over the central plane which causes oscillation. One then takes advantage of the many observable lines associated with a single transition. The temperature is derived through iterations, as in the guess of the kinetic temperature is altered until the modeled spectrum reflects the observed spectrum, Terzieva & Herbst (1998).

Bergin et al. (1994) use Methyl Acetylene (CH_3CCH) as a temperature probe for cloud

cores due its low dipole moment and low opacity. This method makes use of the J(6→5) transition to probe the cloud gas kinetic temperature. However, for densities of $< n_{crit}$ and for $n_{H_2} > 10^2 cm^{-3}$ the kinetic temperature of the gas can be approximated as the excitation temperature of the J(1→0) transition of CO. The excitation temperature of CO can be related to the radiation temperature (the observed temperature) by;

$$T_R = \frac{\lambda^2}{2k}[B_\nu(T_{ex}) - B_\nu(T_{bg})][1 - e^{-\tau_\nu}] \tag{2.18}$$

Where $\tau_\nu >> 1$, T_{bg} is the background temperature of 2.77K and $B_\nu(T)$ is the Planck function.

The kinetic temperature can then be solved for;

$$T_{kin} = \frac{5.54}{ln[(\frac{5.54}{T_R}) + 0.87] + 1} \tag{2.19}$$

2.3.4 Magnetic Field

Within Galactic molecular clouds, it is often interesting to investigate the magnetic field interior to that of the cloud, since it is the magnetic field that can affect the geometry of the cloud and also, slightly more controversially, the star formation process. The molecule used as a probe for the magnetic field is Hydroxyl (OH). Currently the only effective method of observing the magnetic field, or at least its effects of the residual molecules, is that of the Zeeman splitting of the OH energy levels. However in the lower density regions of Dark Clouds, Hydrogen is completely atomic (Crutcher et al. (1981); Crutcher et al. (1993)), hence the Zeeman observations of HI splitting can act as a probe in these regions, but primarily it is the splitting of OH which is useful to the observer. Though it is important to note that the OH emission lines in the direction of Dark Clouds are weak compared to that of continuum emission, hence a reduction in sensitivity is suffered by Zeeman-effect observations.

Briefly, the Zeeman-effect (and hence Zeeman Splitting) is the breaking down of a molecule's energy level degeneracy. Molecules consist of several electronic configurations that have the same energies. Therefore more than one transition may have the same energy of emission. The presence of a Magnetic field breaks this degeneracy and causes the energy levels to become discrete. This is because the effect of the magnetic field is dependent on the electron's quantum number which modifies its energy.

Hence, one may measure the magnetic moment of the OH molecule (from the unpaired electrons) and equate this to the energy of emission and the magnetic field. Through analysis of the total angular momentum and the wave function of the OH, one may define the emission energy from a given Zeeman transition as;

$$\Delta \mathrm{E}_{\mathrm{mag}} = -\mathrm{g}.\mu_{\mathrm{B}}.\mathrm{M}_{\mathrm{F}}.\mathbf{B} \tag{2.20}$$

g is of the order unity and is a function of all the quantum numbers , with the exception of M_F. By division of Planck's constant, one may obtain an expression which equates the magnetic field to a shift in frequency. This shift in frequency arises the net magnetic moment endowed on OH by the presence of an electron pair, measurement of this shift allows one to infer the strength of the magnetic field;

$$\Delta \nu_{\mathrm{mag}} = (\frac{\mathrm{b}}{2}).\mathbf{B} \tag{2.21}$$

More specifically, the initial splitting of the energy levels is referred to as Λ-doubling, this is where previously degenerate levels are split into $\pm\Lambda$ levels, this consitutes a double. The b-value is a constant which is dependent on the molecule which one is observing and has units of Hz $\mu \mathrm{G}^{-1}$.

Chapter 3

Research

As an introduction to utlising CO and online stellar survey data; the first area to be investigated will be based on the paper; Leisawitz et al. (1989), using the J(1→0) transition of CO, the areas around stellar clusters will be observed. The CO survey maps are then attempted to be matched with stellar cluster distributions to see if the clouds occupy the same space as the clusters. The variation of cloud mass with cluster age will then be determined, which yields information as to the lifetimes of Molecular Clouds. The findings of Leisawitz et al. (1989) were that clusters approximately 5Myr have associated molecular clouds of mass $10^4 M_\odot$, clusters older than 10Myr were found to have no associated molecular clouds more massive than $10^3 M_\odot$. Finally, molecular clouds were found to be receding from clusters at 10km s^{-1} and are being destroyed by their interaction with the young stellar populatoins. However, the errors associated with the results were significant. This work will attempt to improve upon the findings by using a larger sample and with newer and more reliable data.

This research will make use of data from the Extended Outer Galaxy Survey (Brunt, Heyer, Douglas and Summers, *in preparation*). EOGS, by definition, is an extension of the FCRAO CO Survey of the Outer Galaxy, Heyer (1996). The cluster data is extracted from the Webda Stellar Cluster Catalogue. There are four stages, of increasing accuracy, of cloud-cluster mass determination;

3.1 H_2 Mass Calculation in Molecular Clouds

There are four methods, of increasing accuracy, to be used to measure the mass of the Hydrogen content of the clouds. The first method makes use to the ^{12}CO isotope using the X-factor method: This method of mass determination has already been touched upon the the main body of the report (see §2.3.1 and §2.3.2). Firstly the ^{12}CO data is extracted from the EOGS catalogue using two methods; a *constant* or variable radius of integration.

The constant radius is, for example, set to 10pc and used for all cluster-cloud associative candidates, where as the variable radius will be dependent on the angular radius of the stellar cluster. The data stored in the EOGS catalogue, is proportional to the intensity in T_A (antenna temperature). Using the following integration, for a velocity centred on V_o (at the stellar cluster centre) over range $\pm\delta v$ for an cylindrical volume of sky of radius r, the intensity of the CO within that area is given by;

$$W_{CO} = \int_{r=0}^{r} (\int_{-\delta v}^{+\delta v} T.dv) dA \tag{3.1}$$

Once a value for W_{CO} is obtained it can be related to the column density of Molecular Hydrogen, N_{H_2}, by the relation:

$$N_{H_2} = W_{CO}.X \tag{3.2}$$

With X $\sim$ 2x10^{20}cm^{-2}. The value of X is independent of the properties of the molecular cloud (e.g. metallicity), Obreschkow & Rawlings (2009). The mass of molecular Hydrogen is obtained via;

$$\mathcal{M}_{H_2} = N_{H_2}.\mathcal{A}_{clus}.m_{H_2} \tag{3.3}$$

Where, $\mathcal{M}_{H_2}$ is the total mass of Hydrogen associated with a stellar cluster (or defined circular radius) of area $\mathcal{A}_{clus}$ for Hydrogen molecules of mass m_{H_2}. This method yields a somewhat crude approximation for the mass of H_2. The next method of determining the H_2 mass is to use generally the same method as above; Firstly one utilises a different isotope of CO, mainly ^{13}CO. Assuming optical thinness for ^{13}CO, the integration expressed in equation 3.1, instead of giving the total number of molecules, gives the number of molecules in the upper (excited) state, N_u. Equating the excitation temperature, T_{ex}, of the ^{13}CO to that of ^{12}CO which gives information to the *total* number of molecules, N_{tot}. This can then be used to calculate the Hydrogen mass.

The third method makes no assumption as to the excitation temperatures,T_{ex}, for the ^{13}CO being equal to that of ^{12}CO. Instead the T_{ex} for ^{13}CO will first be estimated and the Hydrogen mass determined. Then T_{ex} for ^{13}CO will be, within error, known and hence the mass determined and the results compared. This, within error, will present another step up in accuracy due to the reduction in the number of assumptions made and an increase in the number of known, determinable quantities. The final tier of calculation will involve an accurate determination of the optical depth, τ, for the ^{13}CO before calculating the total Hydrogen mass.

3.2 Matching Stellar Clusters to Molecular Clouds

When considering which clusters are to be matched to molecular clouds, it is important to think of the parameter space in which the matching will occur. The parameter space utilised for this work is (l, b, V_{LSR}) and is not physical space. The V_{LSR} for the molecular material and for the cluster need not be equal since there is not a direct relation between V_{LSR} and the heliocentric radius. Though it is noted that one of the tertiary goals of this project is to determine a relationship between these two parameters. Finally, the stellar clusters which *are* to be considered matchable candidates must be young enough so that they may be considered to actually be associated to the cloud and not just an anomaly of the data. An age of $10^6 \sim 10^7$ years for the cluster should be suitable to assume that the association is correct.

Bibliography

Bacmann A., Lefloch B., Ceccarelli C., Castets A., Steinacker J., Loinard L., 2002, A&A, 389, L6

Ballesteros-Paredes J., 2006, MNRAS, 372, 443

Ballesteros-Paredes J., Gómez G. C., Pichardo B., Vázquez-Semadeni E., 2008, ArXiv e-prints

Ballesteros-Paredes J., Hartmann L., Vázquez-Semadeni E., 1999, ApJ, 527, 285

Barnard E. E., 1919a, ApJ, 49, 360

Barnard E. E., 1919b, ApJ, 49, 1

Benjamin R. A., Churchwell E., Babler B. L., Bania T. M., Clemens D. P., Cohen M., Dickey J. M., Indebetouw R., Jackson J. M., Kobulnicky H. A., Lazarian A., Marston A. P., Mathis J. S., Meade M. R., Seager S., 2003, PASP, 115, 953

Bergin E. A., Goldsmith P. F., Snell R. L., Ungerechts H., 1994, ApJ, 431, 674

Bergin E. A., Langer W. D., Goldsmith P. F., 1995, ApJ, 441, 222

Bergin E. A., Tafalla M., 2007, ARA&A, 45, 339

Blitz L., Shu F. H., 1980, ApJ, 238, 148

Blitz L., Williams J. P., 1999, ArXiv Astrophysics e-prints

Bok B. J., Reilly E. F., 1947, ApJ, 105, 255

Burgh E. B., France K., McCandliss S. R., 2007, ApJ, 658, 446

Cambrésy L., Beichman C. A., Jarrett T. H., Cutri R. M., 2002, AJ, 123, 2559

Cazaux S., Tielens A. G. G. M., 2002, ApJL, 575, L29

Crutcher R. M., Troland T. H., Goodman A. A., Heiles C., Kazes I., Myers P. C., 1993, ApJ, 407, 175

Crutcher R. M., Troland T. H., Heiles C., 1981, ApJ, 249, 134

D'Hendecourt L. B., Allamandola L. J., Baas F., Greenberg J. M., 1982, A&A, 109, L12

D'Hendecourt L. B., Allamandola L. J., Greenberg J. M., 1985, A&A, 152, 130

Dickey J. M., Lockman F. J., 1990, ARA&A, 28, 215

Dickman R. L., 1978, ApJS, 37, 407

Du F., Yang J., 2008, ApJ, 686, 384

Elmegreen B. G., 1990a, ApJ, 357, 125

Elmegreen B. G., 1990b, ApJL, 361, L77

Elmegreen B. G., 2000, ApJ, 530, 277

Evans A. S., Kim D. C., Mazzarella J. M., Scoville N. Z., Sanders D. B., 1999, ApJL, 521, L107

Feitzinger J. V., Stuewe J. A., 1984, NASA Conference Publication, 2345, 239

Glover S. C. O., Mac Low M.-M., 2007, ApJ, 659, 1317

Goldsmith P. F., Bergin E. A., Lis D. C., 1997, ApJ, 491, 615

Heger M. L., 1922, Lick Observatory Bulletin, 10, 141

Heyer M. H., 1996, in Latter W. B., Radford Simon J. E., Jewell P. R., Mangum J. G., Bally J., eds, CO: Twenty-Five Years of Millimeter-Wave Spectroscopy Vol. 170 of IAU Symposium, FCRAO CO Survey of the Outer Galaxy. pp 36–+

Hollenbach D., Salpeter E. E., 1971, ApJ, 163, 155

Hollenbach D. J., Werner M. W., Salpeter E. E., 1971, ApJ, 163, 165

Keres D., Yun M. S., Young J. S., 2003a, in Rosenberg J. L., Putman M. E., eds, The IGM/Galaxy Connection. The Distribution of Baryons at z=0 Vol. 281 of Astrophysics and Space Science Library, CO Luminosity Function and the First Estimate for $\mathrm{Omega}_{HI+H_2}.pp33---+$

Keres D., Yun M. S., Young J. S., 2003b, ApJ, 582, 659

Klessen R. S., Ballesteros-Paredes J., Li Y., Mac Low M.-M., 2004, in Lamers H. J. G. L. M., Smith L. J., Nota A., eds, The Formation and Evolution of Massive Young Star Clusters Vol. 322 of Astronomical Society of the Pacific Conference Series, Gravoturbulent Star Cluster Formation. pp 299–+

Larson R. B., 1981, MNRAS, 194, 809

Leisawitz D., Bash F. N., Thaddeus P., 1989, ApJS, 70, 731

Lynds B. T., 1962, ApJS, 7, 1

McKee C. F., 1989, ApJ, 345, 782

Myers P. C., Dame T. M., Thaddeus P., Cohen R. S., Silverberg R. F., Dwek E., Hauser M. G., 1986, ApJ, 301, 398

Obreschkow D., Rawlings S., 2009, MNRAS

Oppenheimer M., Dalgarno A., 1975, ApJ, 200, 419

Russell H. N., 1935, MNRAS, Vol. 95, 610

Simon R., Jackson J. M., Rathborne J. M., Chambers E. T., 2006, ApJ, 639, 227

Skrutskie M. F., Cutri R. M., Stiening R., Weinberg M. D., Schneider S., Carpenter J. M., Beichman C., Capps R., Chester T., Elias J., Huchra J., 2006, AJ, 131, 1163

Snow T. P., McCall B. J., 2006, Annual Review of Astronomy and Astrophysics, 44, 367

Stahler S., Palla F., 2004, The Formation of Stars. Wiley

Swings P., 1937, MNRAS, 97, 212

Swings P., Rosenfeld L., 1937, ApJ, 86, 483

Tafalla M., 2008, Ap&SS, 313, 123

Terzieva R., Herbst E., 1998, ApJ, 501, 207

van der Wiel M. H. D., Shipman R. F., 2008, A&A, 490, 655

van Dishoeck E. F., Black J. H., 1988, ApJ, 334, 771

Walmsley C. M., Ungerechts H., 1983, A&A, 122, 164

Weinreb S., Barrett A. H., Meeks M. L., Henry J. C., 1963, Nature, 200, 829

Willacy K., Williams D. A., 1993, MNRAS, 260, 635